Batteries & Supercaps

Research Article
doi.org/10.1002/batt.202200041

Chemistry Europe
European Chemical Societies Publishing

www.batteries-supercaps.org

Ionic Conductivity versus Particle Size of Ball-Milled Sulfide-Based Solid Electrolytes: Strategy Towards Optimized Composite Cathode Performance in All-Solid-State Batteries

Marvin Cronau[+],[a] Marc Duchardt[+],[a] Marvin Szabo,[a] and Bernhard Roling*[a]

For the fabrication of high-energy and high-power all-solid-state batteries (ASSBs), easily synthesizable solid electrolytes are needed, which enable fast ion transport inside the composite cathode as well as good contacts between cathode active material and solid electrolyte particles. Regarding the latter, the size ratio of the particles inside the composite cathode has to be optimized. Here, we use a wet ball milling process for the synthesis of agyrodite-type $Li_{5.5}PS_{4.5}Cl_{1.5}$ solid electrolyte particles and study the influence of milling time on particle size and ionic conductivity. With longer milling time, both the solid electrolyte particle size and the ionic conductivity decrease, which exert an opposing influence on the cathode performance. We show that a milling time of approximately 2 h leads to an optimum cathode performance, as this time is sufficient for a favorable particle size ratio, while a strong drop of the ionic conductivity of $Li_{5.5}PS_{4.5}Cl_{1.5}$ is avoided.

Introduction

Implementation of metallic lithium (Li) as anode material is regarded as the "holy grail" of Li-ion battery research, as it would allow for unprecedented energy densities. Only, usage of Li metal together with the currently used liquid electrolytes is overly challenging. This is due to the notoriously unstable Li | liquid electrolyte (LE) interface and inevitable Li filament formation upon cycling, which eventually leads to the short-circuiting of the battery.[1,2] However, substitution of the LE by a solid electrolyte (SE) might solve this problem.[3] All-solid-state batteries (ASSBs) are therefore researched intensively as next-generation energy-storage technology.

During the last years, a clear focus of the research community on crystalline argyrodites Li_6PS_5X (X = Cl, Br) as sulfide-based SEs could be observed, since these argyrodites are very well conductive, kinetically quite stable towards both Li metal and cathode active materials, and they do not contain any expensive or hazardous elements.[4–10] Most prominently, Li_6PS_5Cl (LPSC) has been utilized, exhibiting an ionic conductivity of about 3 mS/cm. This conductivity is similar to that of Li_6PS_5Br, but chloride is the more readily available halogenide. Importantly, a further increase in conductivity could recently be achieved by raising the Cl content in $Li_{6-x}PS_{5-x}Cl_{1+x}$, with an optimum conductivity of 8–10 mS/cm observed for the composition $Li_{5.5}PS_{4.5}Cl_{1.5}$ (LPSC+), which thus rivals the well-known $Li_{10}GeP_2S_{12}$.[11–14]

A drawback of any crystalline argyrodite phase is, however, the need for a high-temperature annealing process in order to take full advantage of its conductivity potential.[15,16] This annealing step is not only energy-intensive, but also inextricably linked to an increase in size of the SE particles, which is disadvantageous for the utilization in ASSBs, as explained below. Interestingly, a recent study has shown that the glass ceramic LPSC+ might boast competitive ionic conductivities even without any annealing step, but solely through mechanical milling synthesis.[11] Its conductivity after 6 h of ball milling amounts to about 3 mS/cm, being on a par with the one of crystalline LPSC. Moreover, the higher Cl^- content is likely to reduce the price of LPSC+ compared to LPSC due to the smaller amount of expensive Li_2S needed for the synthesis.[17] However, the sizes of ball-milled LPSC+ particles will certainly be very similar to the ones of other sulfide-based SEs, which were synthesized exclusively by mechanical milling.[18,19]

In a recent study, it was shown that the size ratio $\lambda = d_{CAM}/d_{SE}$, with d_{CAM} and d_{SE} denoting the average diameter of cathode active material (CAM) and the average diameter of the solid electrolyte (SE) particles, respectively, inside the composite cathode of an ASSB should be 2:1 or higher in order to achieve a good AM/SE contact and thus a high utilization of the CAM particles (high capacity).[20] With a typical CAM particle size of less than 5 μm in ASSBs,[21] the SE particle diameter d_{SE} should thus be below 2.5 μm. During typical high-energy dry milling synthesis (HDM) with a ball size in the range of 10 mm, however, such low SE particle diameters are not achievable.[20]

[a] M. Cronau,[+] Dr. M. Duchardt,[+] M. Szabo, Prof. Dr. B. Roling
Department of Chemistry
Philipps-University Marburg
Hans-Meerwein-Str. 4,
35032 Marburg, Germany
E-mail: roling@staff.uni-marburg.de

[+] These authors contributed equally to this work

Supporting information for this article is available on the WWW under https://doi.org/10.1002/batt.202200041

Research Article
doi.org/10.1002/batt.202200041
Chemistry Europe
European Chemical Societies Publishing

Only the utilization of inert solvents, e.g. mixtures of predominantly heptane and a small share of dibutyl ether, together with a smaller ball size of typically 1–3 mm (LWM = low energy wet milling) has proven successful in reducing the particle size of SEs considerably.[20,22–24] Although the need for small SE particles is clearly more urgent for the SE component within the cathode composite than for the SE separator, state-of-the-art ASSBs are already employing SE sheet thicknesses of 30 µm and a further reduction is likely. Common particle size distributions with a considerable amount of particles having diameters >20 µm are therefore not viable for the separator layer either.[4,18]

Unfortunately, extended LWM exceeding 40 h leads to a significant reduction of ionic conductivity of the SE to about 1/3 of the original value, which has been attributed to increased particle boundary resistances and inclusion of residual solvent.[20,25] Thus, there is an opposing effect of the milling time on the SE particle size and on the ionic conductivity, and consequently there should be an optimum milling time, which is sufficiently long for reducing the SE particle size, but adequately short for avoiding a strong drop of the ionic conductivity, see schematic illustration in Figure 1. Consequently, we have carried out a systematic study on the influence of low-energy wet milling (LWM) on the particle size d_{SE} and the ionic conductivity of two promising SEs, namely of glass-ceramic LPSC+ (gc-LPSC+) and of microcrystalline LPSC+ (µc-LPSC+). Furthermore, we study the performance of SEs in ASSBs and link their performance to $\lambda = d_{CAM}/d_{SE}$ and the ionic conductivity of the SE.

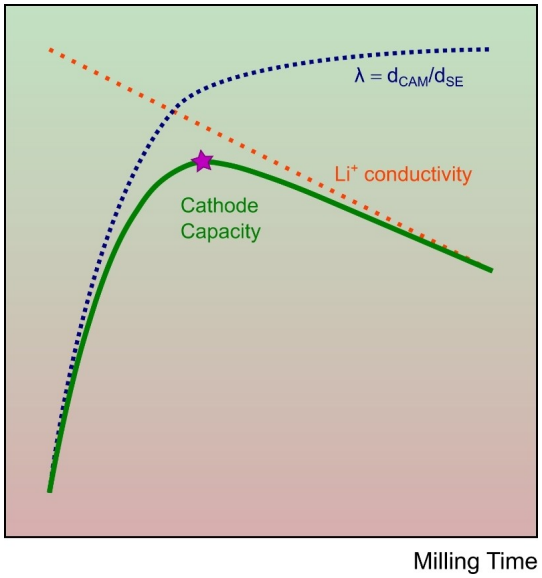

Figure 1. Schematic illustration of the opposing effect of milling time on the ionic conductivity of the solid electrolyte (orange dotted line) and on the size ratio λ of the cathode active material particles to the solid electrolyte particles (blue dotted line). This opposing effect should lead to an optimum milling time for achieving a maximum cathode capacity (green line).

Results and Discussion

In a first step, both glass-ceramic $Li_{5.5}PS_{4.5}Cl_{1.5}$ (gc-LPSC+) and microcrystalline $Li_{5.5}PS_{4.5}Cl_{1.5}$ (µc-LPSC+) were synthesized by means of high-energy dry milling (HDM) with an additional annealing step for obtaining µc-LPSC+. In the case of gc-LPSC+, the utilization of 10 mm balls (largest balls available) resulted in the highest achievable conductivity value of 2.5 mS/cm. The ionic conductivity of µc-LPSC+, on the other hand, was governed by the annealing process and did not depend on the ball size.

In a second step, the as-synthesized powders of both gc-LPSC+ and µc-LPSC+ were subjected to a low-energy wet milling (LWM) step to reduce the particle size. As depicted in Figure 2, independent of the ball size, the conductivities of both gc-LPSC+ and µc-LPSC+ drop with increasing milling time. Interestingly, the ball size does not have a profound impact on the conductivity drop. However, the drop is clearly steeper for µc-LPSC+ than for gc-LPSC+, so that the difference in conductivity between these materials becomes smaller with increasing milling time. The X-ray diffractograms obtained after different wet milling times shown in Figure S2 suggest that a partial amorphization during wet milling is a likely reason for the conductivity drop. Furthermore, our results indicate that

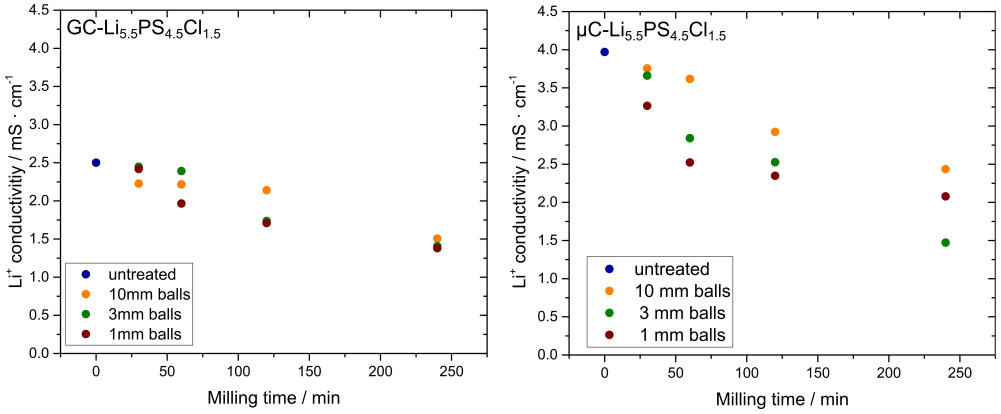

Figure 2. Time-dependent evolution of ionic conductivity of gc-LPSC+ and µc-LPSC+ samples milled with balls of different sizes in the low energy wet milling (LWM) step.

the annealing transformation of gc-LPSC+ to μc-LPSC+ does not lead to any advantage for ASSB applications, if low-energy wet milling (LWM) is carried out subsequently. A recent study of the Janek group shows that crystalline SEs suffer from additional, rather unexpected, disadvantages compared to their glass-ceramic counterparts of the same stoichiometry.[26] Both the higher electronic conductivity and the stronger tendency to contact loss upon cycling lead, in sum, to a worse long-term performance of microcrystalline SEs in ASSBs.

Therefore, we regard an energy-intensive sintering process for the synthesis of μc-LPSC+ particles as dispensable and continued our study exclusively with the more promising gc-LPSC+.

In Figure 3, we show SEM images of the final gc-LPSC+ powders, illustrating the influence of the ball size used during LWM on the size of the SE particles. After HDM synthesis, the average SE particle size is about 20 μm, see Figure 3a). After LWM with 10 mm balls, there is a drastic reduction of the average particle size, see Figure 3b). However, some very large chunks (Ø ≈ 20 μm) clearly remain. Usage of 3 mm balls during LWM leads to a further reduction of the particle size, see Figure 3c), with an average particle size of 1.6 μm, however with the sizes of individual particles exceeding 5 μm. Only with the smallest ball size of 1 mm, a very narrow size distribution is achieved with an average particle size of 1.0 μm (Figure 3d). This average SE particle size below 1 μm is urgently needed to reach adequate properties in composite cathodes and, thus, optimal cell performances.[4,20] This holds particularly true when using small average CAM particle sizes as we do in this study with 3.5 μm.

In a next step, we examined the influence of the milling time on the particle size, when subjecting pristine gc-LPSC+ to a LWM step with 1 mm balls. As can be seen from Figure 4a), after 30 min, the particle size of pristine gc-LPSC+ (Figure 3a) is drastically reduced from 4 μm (untreated material) to 1.8 μm. A further comminution to an average particle size of 1 μm can be reached after 1 h and after 2 h of milling time. However, no significant further reduction of particle size is observed after 4 h. Therefore, a milling time of 1–2 h is sufficient for reducing the SE particle size to sufficiently low values.

Next, in order to evaluate the optimum milling time for a high performance of composite cathodes (Figure 1), battery cells were constructed with $LiNi_{0.85}Co_{0.10}Mn_{0.05}$ (NCM-85|10|05) as CAM (Figure 5) and gc-LPSC+ after different LWM durations as SE in the composite cathode. gc-LPSC+ without any subsequent LWM was chosen for the SE separator layer in order to rule out any influence of the separator on the battery performance. In foil was used as anode material, so that the ASSBs differed exclusively with regard to the solid electrolyte particles integrated in the composite cathodes.

Without any LWM treatment, a first discharge capacity of 187 mAh/g was obtained in a benchmark cell cycled at a rate of 0.1 C (Figure S3). With the same type of battery cycled at 0.6 C, only 152 mAh/g were achieved in the first discharge at

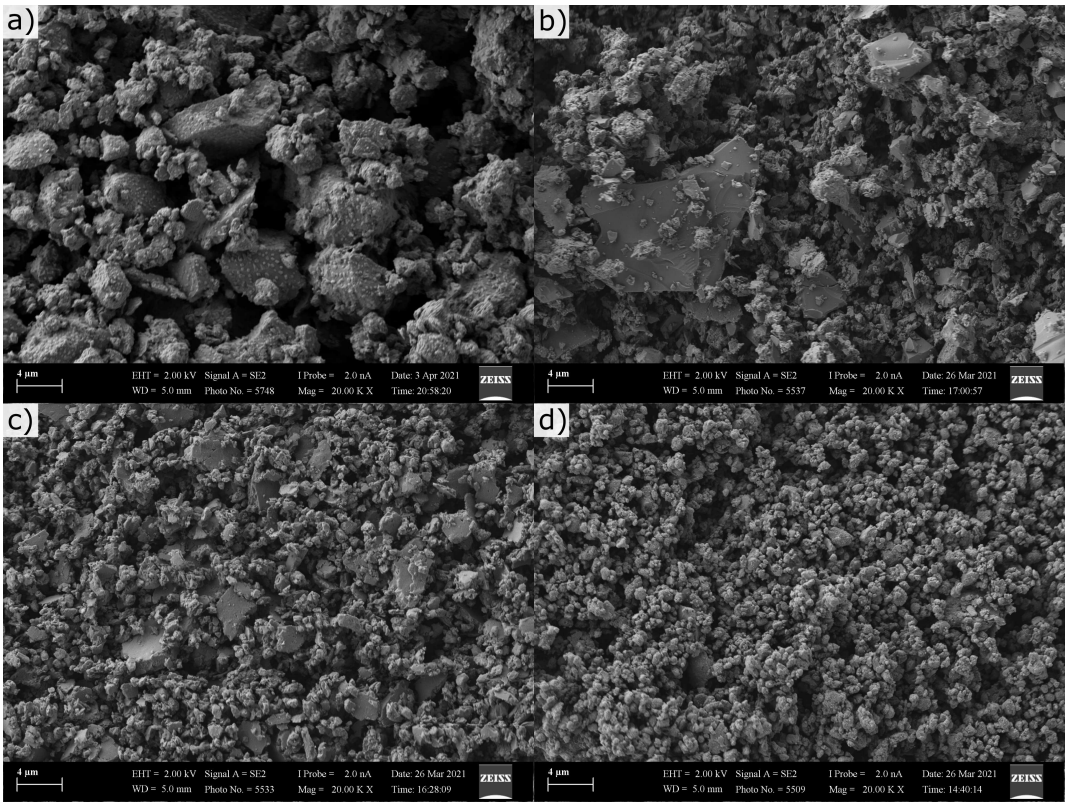

Figure 3. SEM images of gc-LPSC+ powders after low energy wet milling (LWM) at 200 rpm for 4 h, but with different ball sizes. a) pristine – without any LWM treatment, b) LWM with 10 mm balls, c) LWM with 3 mm balls, d) LWM with 1 mm balls. The scale bars are 4 μm.

Research Article
doi.org/10.1002/batt.202200041

Chemistry Europe
European Chemical Societies Publishing

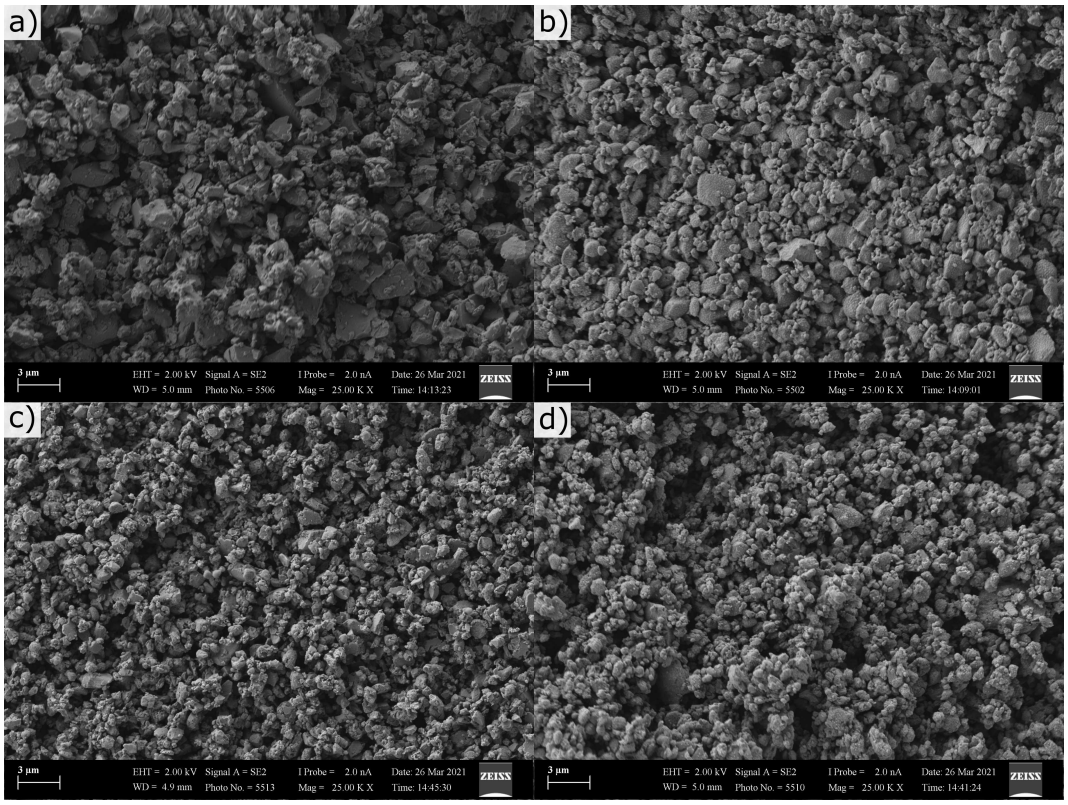

Figure 4. SEM images of gc-LPSC+ powders after low energy wet milling (LWM) at 200 rpm ($Ø_{balls}$ = 1 mm) for different milling times. a) 0.5 h, b) 1 h, c) 2 h, d) 4 h. The scale bars are 3 µm.

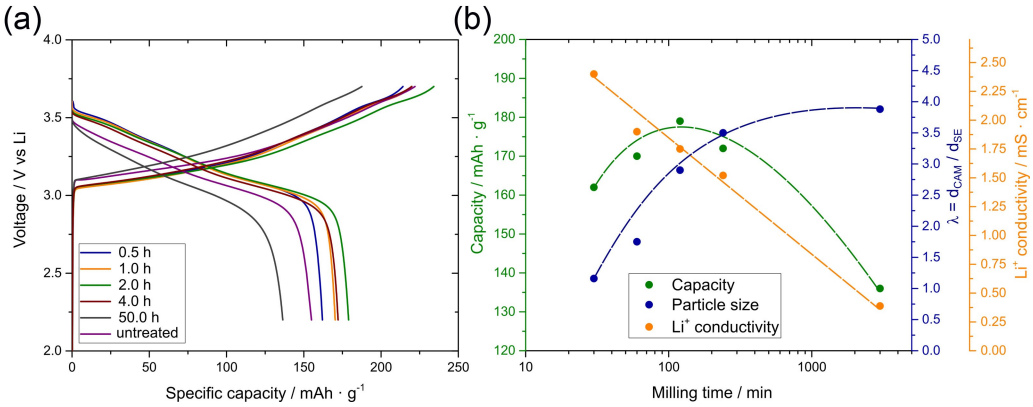

Figure 5. a) Comparison of six In-based cells cycled at RT and at a rate of 0.6 C (1.27 mA/cm^2) using a stack pressure of 98 MPa. The gc-LPSC+ powders inside the composite cathode were synthesized via LWM treatment with different milling times. b) Dependence of the attained first discharge capacities of the batteries on the LWM milling time of the gc-LPSC+ SE in the composite cathode (0.5–50 h). In addition, the ionic conductivities and the particle size ratio λ are plotted.

an overpotential of 100 mV, which act as benchmark values, see Figure 5(a). After a short LWM duration of 30 min, an increased capacity of 160 mAh/g was obtained at a reduced overpotential of 60 mV, which can be ascribed to a better CAM/SE contact due to the reduced SE particle size. Further improvements of the cell capacity are achieved after LWM durations of 1 h and 2 h, respectively. The maximum discharge capacity during the first cycle at a rate of 0.6 C was 179 mAh/g, achieved after 2 h LWM of the SE inside the cathode. However, after a LWM duration of 4 h, the overpotential rises to a value of 80 mV, linked to a lower first discharge capacity of 172 mAh/g. After an extended LWM treatment of 50 h, the first discharge capacity drops below 140 mAh/g. This drop in capacity after extended LWM treatment is attributed to the reduction of the ionic conductivity of the particles overcompensating the improved CAM/SE contact.

In Figure 5(b), we summarize our results for the size ratio $\lambda = d_{CAM}/d_{SE}$, for the ionic conductivity of the SE particles, and

Research Article
doi.org/10.1002/batt.202200041

for the ASSB capacity. The results confirm the opposing effect of CAM/SE contact and of the SE ionic conductivity on the cathode performance as proposed in the schematic illustration in Figure 1.

After 2 h of LWM treatment, the size ratio λ is around 2.5, which should be sufficient for a good CAM | SE contact.[20] Thus, longer LWM treatment should neither result in better CAM | SE contact nor in significant changes of the tortuosities of the ion transport pathways inside the composite cathode. Consequently, the increasing overvoltage when increasing the LWM treatment to 50 h should mainly result from the drop in ionic conductivity. The rate of 0.6 C corresponds to a current density of $j = 1.27$ mA/cm^2. In this case, the overvoltages observed after 2 h LWM treatment, $h_{2h} = 60$ mV, and after 50 h LWM treatment, $h_{250h} = 150$ mV correspond to the overall battery resistances of $R_{2h} = h_{2h}/j = 47\ \Omega\,cm^2$ and $R_{50h} = h_{50h}/j = 118\ \Omega\,cm^2$, respectively. The thickness of the SE separator is 500 μm in both cases, which results in a resistance of $R_{separator} = 20\ \Omega\,cm^2$. The resistance of the interface between the In–Li anode and a sulfide-based SE was found to be in the range of $R_{In-Li|SE} \approx 10\ \Omega\,cm^2$.[27] Subtracting $R_{separator}$ and $R_{In-Li|SE}$ from R_{2h} and R_{50h}, respectively, one obtains cathode resistance of $R_{cathode,2h} \approx 17\ \Omega\,cm^2$ and $R_{cathode,50h} \approx 88\ \Omega\,cm^2$. The ratio of these values is about 1/5, which is very close to the inverse ratio of the ionic conductivities measured after 2 h and 50 h LWM treatment (1.73 mS/cm and 0.36 mS/cm, ratio ≈ 4.8). This confirms our conclusion that the increasing overvoltage during extended LWM treatment results mainly from the drop in ionic conductivity.

Conclusion

In summary, we have shown that a two-step milling process, high-energy dry milling (HDM) followed by low-energy wet milling (LWM) is a promising route for the synthesis of highly conductive solid electrolytes with small particle sizes. The wet milling time should be long enough for increasing the size ratio $\lambda = d_{CAM}/d_{SE}$ to values > 2, but adequately short for avoiding a strong drop of the ionic conductivity of the SE particles. In the case of argyrodite-based gc-LPSC+, a LWM time of 2 h and ball diameters of 1 mm led to solid electrolyte particles with high performance in ASSBs. Virtually full utilization of the theoretical capacity of the CAM particles and low overpotentials were observed in lab-scale batteries at room temperature and at a cycling rate of 0.6 C. Thus, the two-step milling process should make the application of any subsequent annealing steps for the solid electrolyte dispensable.

Experimental Section

Material synthesis

For the synthesis of gc-LPSC+, stoichiometric amounts of LiCl (99.9%, Sigma Aldrich), Li_2S (99.99%, Sigma Aldrich) and P_2S_5 (99%, Sigma Aldrich) were filled into a zirconia grinding bowl with a volume of 20 mL. The mixture was milled with 10 zirconia balls (Ø = 10 mm) using a Pulverisette 7 premium line (Fritsch) at 850 rpm for 8.25 h (HDM). Afterwards, the resulting SE powder was ground in an agate mortar to obtain the final product.

c-LPSC+ was synthesized by annealing a pellet of gc-LPSC+ inside a quartz glass ampule at 550 °C for 12 h at a heating rate of 60 °C/h. The pellet was ground in an agate mortar to obtain the final product.

Particle size reduction

The SE powders of gc-LPSC+ and c-LPSC+ were filled into the same zirconia grinding bowl as used for the HDM step for the ensuing LWM step. To this end, zirconia grinding balls with 3 different diameters were used: either 10 mm (10 balls) or 3 mm or 1 mm (30 g, respectively). Independent of the ball size, a mixture of heptane (4.0 mL) and dibutyl ether (0.8 mL) was added. The mixture was milled at 200 rpm between 30 and 240 min (30 min milling time, 30 min rest). The resulting suspensions were dried under vacuum. The obtained powders were ground in an agate mortar to obtain the final products.

Conductivity measurements

The Li^+ conductivity measurements were performed inside a CompreDrive automated die press (rhd instruments). 105 mg of the as-prepared powders were pressed to a pellet by applying a fabrication pressure of 394 MPa for 60 sec. Afterwards, the pressure was completely released. During the subsequent impedance measurements, a stack pressure of 98 MPa was applied. The measurements were carried out with a PGSTAT302 N potentiostat (Metrohm Autolab). The frequency range extended from 10^5 to 10^1 Hz and the AC voltage was set to 10 mV.

$LiNbO_3$ coating of NMC-85 | 05 | 10

The $LiNbO_3$ (LNO) coating was carried out according to a literature protocol.[28] A 1 M stock solution of LiOEt in EtOH was mixed with $Nb(OEt)_5$ in a vial inside a glovebox. 6 g of CAM (NCM-85 | 10 | 05, provided by BASF SE) with a theoretical specific discharge capacity of 200 mAh/g was added to the solution, and the vial was transferred to an ultrasonic bath outside the glovebox. The bath was heated to 75 °C and after complete evaporation of EtOH, the resulting material was carefully ground in an agate mortar and calcined in air at 400 °C for 1 h (heating rate: 20 °C/h).

Preparation of electrode composites

The cathode composite powder was prepared by mixing the different as-prepared SEs with LNO@NMC and carbon nanofibers (Nanografi) in an agate mortar in a weight ratio of 30 : 70 : 3.

Fabrication of all-solid-state battery (ASSB) with In anode and Galvanostatic cycling

For fabricating the solid electrolyte separator of the ASSB, 100 mg of LPSC+ were filled into a polyether ether ketone (PEEK) mold (Ø = 10 mm) and a pressure of 294 MPa was applied for 60 seconds. For the solid electrolyte separator, we used LPSC+ after the HDM synthesis without any subsequent LWM treatment. Subsequently, 13 mg of the cathode composite and an In sheet (25 mg, pre-pressed at 300 MPa) were spread on both sides of the SE separator layer. The resulting stack was densified at a pressure of 392 MPa with two stainless steel pistons. The galvanostatic cycling experi-

ments were carried out at ambient temperature (25 °C) and at pressures of 98 MPa, respectively. The upper and low cutoff potentials were chosen as 3.7 V and 2.2 V, respectively, vs. In/Li.

Acknowledgements

M. Duchardt acknowledges support through a scholarship of the Marburg Research Academy (MARA). The NMC-85|05|10 particles were kindly provided by BASF SE. Open Access funding enabled and organized by Projekt DEAL.

Conflict of Interest

The authors declare no conflict of interest.

Data Availability Statement

Research data are not shared.

Keywords: all-solid-state battery · ball milling · capacity optimization · composite cathode · glass-ceramic solid electrolyte

[1] A. Kushima, K. P. So, C. Su, P. Bai, N. Kuriyama, T. Maebashi, Y. Fujiwara, M. Z. Bazant, J. Li, *Nano Energy* **2017**, *32*, 271–279.
[2] S. Li, M. Jiang, Y. Xie, H. Xu, J. Jia, J. Li, *Adv. Mater.* **2018**, *30*, 1706375.
[3] G. Liu, W. Weng, Z. Zhang, L. Wu, J. Yang, X. Yao, *Nano Lett.* **2020**, *20*, 6660–6665.
[4] Y. G. Lee, S. Fujiki, C. Jung, N. Suzuki, N. Yashiro, R. Omoda, D. S. Ko, T. Shiratsuchi, T. Sugimoto, S. Ryu, J. H. Ku, T. Watanabe, Y. Park, Y. Aihara, D. Im, I. T. Han, *Nat. Energy* **2020**, *5*, 299–308.
[5] A. Banerjee, X. Wang, C. Fang, E. A. Wu, Y. S. Meng, *Chem. Rev.* **2020**, *120*, 6878–6933.
[6] J. M. Doux, H. Nguyen, D. H. S. Tan, A. Banerjee, X. Wang, E. A. Wu, C. Jo, H. Yang, Y. S. Meng, *Adv. Energy Mater.* **2020**, *10*, DOI 10.1002/aenm.201903253.
[7] J. Kasemchainan, S. Zekoll, D. Spencer Jolly, Z. Ning, G. O. Hartley, J. Marrow, P. G. Bruce, *Nat. Mater.* **2019**, *18*, 1105–1111.
[8] Q. Zhao, M. Avdeev, L. Chen, S. Shi, *Sci. Bull.* **2021**, *66*, 1401–1408.
[9] Q. Zhao, L. Zhang, B. He, A. Ye, M. Avdeev, L. Chen, S. Shi, *Energy Storage Mater.* **2021**, *40*, 386–393.
[10] M. Cronau, M. Szabo, B. Roling, *Mater. Adv.* **2021**, *2*, 7842–7845.
[11] W. Dum Jung, J.-S. Kim, S. Choi, S. Kim, M. Jeon, H.-G. Jung, K. Yoon Chung, J.-H. Lee, B.-K. Kim, J.-H. Lee, H. Kim, *Nano Lett.* **2020**, *20*, 2303–2309.
[12] L. Zhou, K. H. Park, X. Sun, F. Lalère, T. Adermann, P. Hartmann, L. F. Nazar, *ACS Energy Lett.* **2019**, *4*, 265–270.
[13] P. Adeli, J. D. Bazak, K. H. Park, I. Kochetkov, A. Huq, G. R. Goward, L. F. Nazar, *Angew. Chem. Int. Ed.* **2019**, *58*, 8681–8686; *Angew. Chem.* **2019**, *131*, 8773–8778.
[14] S. V. Patel, S. Banerjee, H. Liu, P. Wang, P. H. Chien, X. Feng, J. Liu, S. P. Ong, Y. Y. Hu, *Chem. Mater.* **2021**, *33*, 1435–1443.
[15] C. Yu, S. Ganapathy, J. Hageman, L. Van Eijck, E. R. H. Van Eck, L. Zhang, T. Schwietert, S. Basak, E. M. Kelder, M. Wagemaker, *ACS Appl. Mater. Interfaces* **2018**, *10*, 33296–33306.
[16] M. Cronau, M. Szabo, C. König, T. B. Wassermann, B. Roling, *ACS Energy Lett.* **2021**, *6*, 3072–3077.
[17] M. Duchardt, M. Diels, B. Roling, S. Dehnen, *ACS Appl. Energ. Mater.* **2020**, *3*, 6937–6945.
[18] S. Spannenberger, V. Miß, E. Klotz, J. Kettner, M. Cronau, A. Ramanayagam, F. di Capua, M. Elsayed, R. Krause-Rehberg, M. Vogel, B. Roling, *Solid State Ionics* **2019**, *341*, 115040.
[19] M. Kroll, M. Duchardt, S. L. Karstens, S. Schlabach, F. Lange, J. Hochstrasser, B. Roling, U. Tallarek, *J. Power Sources* **2021**, *505*, 230064.
[20] T. Shi, Q. Tu, Y. Tian, Y. Xiao, L. J. Miara, O. Kononova, G. Ceder, *Adv. Energy Mater.* **2020**, *10*, 1902881.
[21] F. Strauss, T. Bartsch, L. de Biasi, A. Y. Kim, J. Janek, P. Hartmann, T. Brezesinski, *ACS Energy Lett.* **2018**, *3*, 992–996.
[22] T. Asano, S. Yubuchi, A. Sakuda, A. Hayashi, M. Tatsumisago, *J. Electrochem. Soc.* **2017**, *164*, A3960–A3963.
[23] A. Sakuda, K. Kuratani, M. Yamamoto, M. Takahashi, *J. Electrochem. Soc.* **2017**, *164*, A2474–A2478.
[24] C. Park, S. Lee, K. Kim, M. Kim, S. Choi, D. Shin, *J. Electrochem. Soc.* **2019**, *166*, A5318–A5322.
[25] P. Minnmann, L. Quillmann, S. Burkhardt, F. H. Richter, J. Janek, *J. Electrochem. Soc.* **2021**, DOI 10.1149/1945-7111/abf8d7.
[26] S. Wang, W. Zhang, X. Chen, D. Das, R. Ruess, A. Gautam, F. Walther, S. Ohno, R. Koerver, Q. Zhang, W. G. Zeier, F. H. Richter, C. Nan, J. Janek, *Adv. Energy Mater.* **2021**, 2100654.
[27] A. L. Santhosha, L. Medenbach, J. R. Buchheim, P. Adelhelm, *Batteries & Supercaps* **2019**, *2*, 524–529.
[28] A.-Y. Kim, F. Strauss, T. Bartsch, J. H. Teo, T. Hatsukade, A. Mazilkin, J. Janek, P. Hartmann, T. Brezesinski, *Chem. Mater.* **2019**, *31*, 9664–9672.

Manuscript received: January 21, 2022
Revised manuscript received: February 24, 2022